A Latching Ferrite Rotary-Field Phase Shifter

CHARLES R. BOYD, JR.
Microwave Applications Group, Santa Maria, California, U. S. A.

For more than two decades ferrite rotary–field phase shifters have offered highly accurate reciprocal phase control at moderate to high microwave power levels, at the expense of continuous current excitation. This paper presents the concept, basic design considerations, and initial data for the first realizations of latching versions of the ferrite rotary–field phase shifter. These versions operate at remanent magnetization and provide frequency–independent and temperature–independent phase changes using state–independent switching pulses, with substantial reduction of control power for low or moderate switching rates. However, the changes in configuration desirable for latching operation imply slightly larger rms phase errors and a reduced capability for average r–f power handling. Data are presented for laboratory–type C–Band and S–Band units.

I. Introduction

In 1947 Fox [1] described a "rotary–vane" microwave phase changer in circular waveguide, in which two 90° differential phase sections (quarter–wave plates) of fixed angular orientation were separated by a 180° differential phase section (half–wave plate) of rotatable orientation. In his paper, Fox presented a mathematical analysis of the operating principal, and pointed out that the approach was analogous to a well–known optical configuration of much earlier vintage. Cacheris [2] applied the concept to a ferrite–loaded waveguide and in 1954 showed experimental results for a device operating at X–Band; his configuration evidently used a rotatable two–pole transverse magnetic bias field to generate the required 180° differential phase section. A thorough analysis of Fox's basic configuration was published in 1971 by Sultan [3], who calculated and plotted the amplitude and phase errors that would be expected as a result of deviations from optimum differential phase in the quarter–wave and half–wave plates. Sultan also showed measured data for a structure using a ferrite tube and a simple drive stator with fixed–orientation fourpole bias field, and concluded that the probable insertion loss was about 0.4 dB.

Concurrent with (but unrelated to) the publication of Sultan's paper, the author's company began delivery of the first set of high–power "rotary–field" S–Band ferrite phase shifters for use in the USAF/Westinghouse E–3A AWACS radar antenna. This design evolved over a period of about a year of concentrated effort, and was based on earlier work on the same generic type of configuration [4]. Data on the AWACS–type duplexing phase control component were presented [5] in the following year. These data included insertion loss and return loss envelopes of a phase–scanned unit, as well as a typical plot of phase deviation from command angle over a 450° phase range, showing the effect of hysteresis. Since that time, the geometry has been used in a number of antennas with single–axis phase scanning, where high phase accuracy and/or the ability to handle moderate amounts of r–f power is important. A summary of performance statistics on a group of medium power (40 KW. peak, 600W. average) S–Band rotary–field phase shifters is available from the literature [6]; these units operated with typical rms phase errors on the order of 0.75° and average insertion loss around 0.35 dB.

All of the rotary–field ferrite phase shifters reported to date have required continuous current in the quiescent condition, as well as higher voltages and currents in the transient condition switching from one quiescent phase value to another. The novel variant described in this paper differs from previous configurations by eliminating the need for continuous current once a desired insertion phase value has been attained. The material presented below briefly reviews the principle of operation for the conventional rotary–field phase shifter, and discusses the changes in materials and configuration that are necessary to promote latching, i.e. quiescent operation at remanent magnetic bias field. The concept of a total flux Φ–plane is introduced to depict graphically the magnitude and angular orientation of the transverse fourpole magnetic bias field in the ferrite, and projections of transient magnetizing current in the sine and cosine windings are indicated for a few cases of excitation at different command angles, based on the Φ–plane model. Finally, data are presented for a laboratory models of latching rotary–field phase shifters operating at C–Band and S–Band.

II. Basic configuration

The basic functional diagram of the rotary–field phase shifter is sketched in Figure 1. A central rotatable half–wave plate is coupled at each end to fixed quarter–wave plates, which in turn couple to transducers to waveguides

Fig. 1. Functional block diagram for a ferrite rotary–field phase shifter.

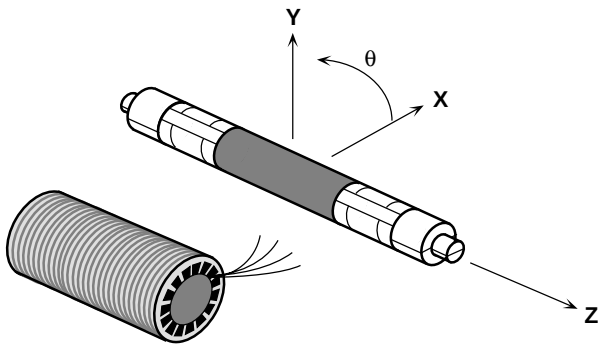

Fig. 2. Sketch of internal parts of a typical ferrite rotary–field phase shifter, showing drive stator with ferrite rod, dielectric quarter–wave plates, and transducers prior to metallization.

or other transmission structures. Figure 2 sketches a practical realization consisting of a central ferrite cylinder which completely fills a circular waveguide and which is coupled at each end to ceramic dielectric assemblies that inhomogeneously fill the waveguide. These dielectric quarter–wave plate sections convert linear polarization incident at either end into circularly polarized TE_{11} mode waves at the interface with the ferrite section. Beyond the dielectric quarter–wave plates are transducers coupling the circular waveguide to ordinary rectangular guide, and at the same time absorbing any energy cross–polarized to the propagating wave orientation. The ferrite is biased with a transverse fourpole magnetic field to a level that creates a birefringence of 180° differential phase (i.e. a half–wave plate). This bias field is produced by "sine" and "cosine" windings placed on a frame that resembles a motor stator, located outside the metallic waveguide wall next to the ferrite. Each winding produces a transverse fourpole magnetic field in the ferrite rod, and the windings are interlaced such that the principal axes of the fourpole bias field can be rotated to any angle by proper setting of the currents in the two windings. Ideally, the sine winding is arranged to produce a radial magnetic flux density B_s around the periphery of the rod with a dependence

$$B_s = B_{s0}\, sin(2\theta) \tag{1}$$

with the cosine winding flux density B_c as

$$B_c = B_{c0}\, cos(2\theta). \tag{2}$$

Now define the electrical angle ϕ and let the magnitudes of B_{s0} and B_{c0} vary as $B_0\, sin(\phi)$ and $B_0\, cos(\phi)$, respectively. Neglecting nonlinear magnetic effects, the superposition of the fields for the two windings will be

$$B = B_0\, (sin(\phi)sin(2\theta) + cos(\phi)cos(2\theta))$$

$$B = B_0\, cos(2\theta - \phi). \tag{3}$$

Thus a change ϕ_a degrees in the electrical angle parameter will cause a mechanical rotation of the ferrite half–wave plate fourpole transverse magnetic bias field by $\phi_a/2$ degrees. Since the r–f insertion phase changes by twice the rotation angle of the half–wave plate, it follows that changes in the winding current distribution angle parameter ϕ correlate exactly with the (r–f frequency independent) microwave insertion phase angle changes.

Conventional rotary–field phase shifters use a stack of thin metallic laminations as the core of the stator on which the windings are placed. Also, an air gap is incorporated between the stator and the metallized ferrite rod, introducing a demagnetizing field and allowing the bias field level to be controlled (with uncertainties caused by hysteresis and saturation effects) by applied continuous currents $I_{max}\sin\phi$ and $I_{max}\cos\phi$ in the sine and cosine windings, respectively. From elementary motor theory, the control power needed to develop a given mmf for a steady bias field is inversely proportional to the weight of copper in the windings, and therefore the stator size and weight are reduced only at the penalty of higher drive power in the quiescent condition. While steps can be (and are) taken to decrease the required mmf by reducing the demagnetizing effects of the air gap between the stator and the ferrite rod, the lowered mmf is attained only at the expense of greater hysteresis effects in the phase shifter output. Eddy currents induced during switching can be reduced by sputtering a thin film metallic waveguide wall directly onto the ferrite rod, allowing practical switching in 100μsec. or less to be achieved. Because the amount of ferrite needed is only enough to produce 180° of phase difference, the unit is capable of attaining low insertion loss. Low r–f power dissipation plus good heat transfer by conduction through the metal drive stator allow moderate average power handling without excessive temperature rise. The peculiar modulo–360° operation allows phase to be changed continuously and without limit in the same direction, so that small frequency offsets can be produced.

III. Latching Considerations

For quiescent operation at remanent magnetization, important changes are necessary in the design of the bias magnetic circuit. The air gap between the microwave ferrite rod and the stator must be reduced so that its demagnetizing effects are acceptably small. At remanent operation, the line integral of the magnetic field around any closed path must equal zero. Consequently it is desirable to use a square–loop ferrite material for the stator core, so that a small negative mmf is available to overcome the positive mmf from the field in the air gap. Because the ferrite core material is brittle, the number of slots that can be realized practically will be smaller than for a metal core. Theory indicates that the attainable rms error increases with decreasing number of slots, therefore latching rotary–field phase shifters ought to have higher rms error levels than similar nonlatching units. There are also significant differences between the bias magnetic field distribution of the latching rotary–field phase shifter compared with that of other ferrite phase shifters.

The most familiar types of ferrite latching phase shifter

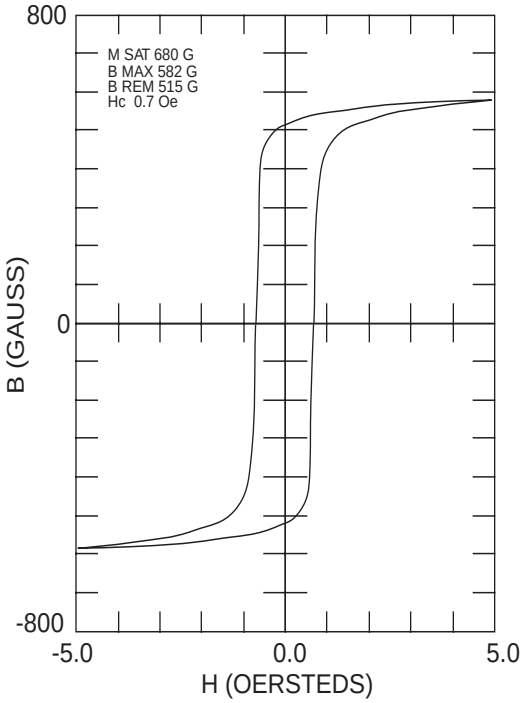

Fig. 3. Typical hysteresis characteristics for a ferrite (garnet) material toroid.

are the nonreciprocal transverse–field axial toroid configuration and the reciprocal longitudinal–field dual–mode geometry. In both these types, the biasing magnetic flux density *B* is essentially uniform in magnitude throughout the cross–section of the r–f ferrite, and the insertion phase is controlled by varying the intensity of that field from maximum negative remanence through maximum positive remanence. The relationship between the biasing flux density *B* and the biasing magnetic field *H* can be represented by a hysteresis loop of the general shape shown in Figure 3. (Note that the *measurement* of hysteresis loop characteristics usually involves plotting the excitation current in a primary coil wound on a toroid against the integrated induced voltage in a secondary coil. The measured current is related to the line integral of the magnetic field *H*, and the integrated voltage to the surface integral of the flux density *B*. Values for *B* and *H* are calculated by dividing out the cross–sectional area and mean path length of the toroid, respectively.) The available range of phase shift for these types of device is determined both by the design of the device and by the major–loop remanence values of *B*. The operating point for any desired phase value is usually set by partial switching of flux away from one of the major–loop limits that is specified to be a reset reference.

The situation for the latching rotary–field phase shifter is dramatically different. First of all, the biasing flux density *B* in the microwave ferrite has a transverse fourpole distribution, so that the field is clearly not uniform in either magnitude or direction. While hysteresis characteristics are still measured, the fact of nonuniform field distribution tends to "soften" the saturation corners compared with those of a simple toroid. This phenomenon is shown quantitatively in Figure 4, which compares the shape of measured hysteresis loops for a

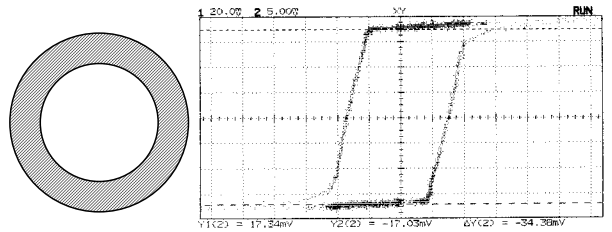

a. Simple toroid cross–section and hysteresis loop

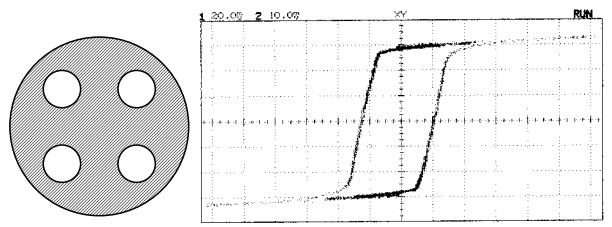

b. Four–window configuration cross–section and hysteresis loop

Fig. 4. Measured hysteresis loops for a simple toroid and for a four–window configuration producing a fourpole field.

simple toroid and for a four–window configuration, wound to produce a fourpole field. Both samples were fabricated from the same 3200 Gauss lithium ferrite material.

From equations (1) – (3), a given distribution of *B* can be produced by excitation of the sine winding, of the cosine winding, or by a combination of excitations of both windings. As Figure 5 indicates, the field distributions created by excitations of the sine winding and of the cosine winding are in principle identical but have an angular displacement of 45 degrees from each other and are orthogonal. Next, the insertion phase is set by selecting the angular orientation of the *B* field pattern, relative to a reference angle. Finally, the magnitude of the *B* field pattern has an optimum value, i.e. the value that sets the half–wave plate differential phase to minimize deviations from 180° over the frequency band of interest. This value is independent of the phase state setting, and minimizes the insertion loss and its modulation over the entire range of phase states.

The conditions stated above can be displayed graphically by the presentation shown in Figure 6. Here the parameter graphed is the integrated total flux value Φ of

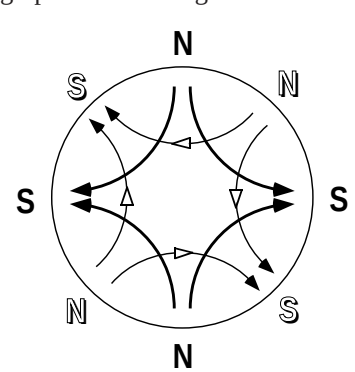

Fig. 5. Typical interlaced transverse fourpole magnetic bias field patterns produced in the ferrite rod by excitation of sine and cosine windings.

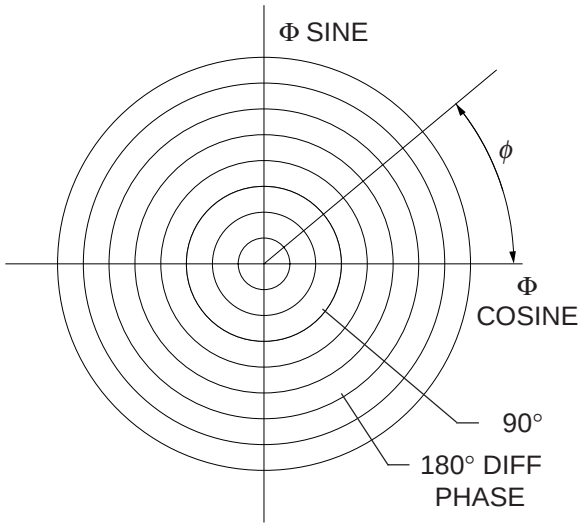

Fig. 6. Φ–plane mapping of resultant total fourpole field flux created by simultaneous transient excitation of sine and cosine windings. The angle ϕ represents a typical case, and the circles map contours of constant differential phase in the ferrite rod.

the fourpole B field, a quantity which can be calculated by

$$\Phi = \int_S B \cdot ds \quad , \tag{4}$$

where S is the aggregate surface for two similar poles of the fourpole distribution, e.g. the two North poles. Consequently, it is meaningful to display Φ values on an ordinary two–dimensional plot. The component of Φ resulting from cosine winding excitation may be plotted along the horizontal axis, and the component of Φ caused by sine coil excitation along the vertical axis, in the usual manner. Then values of Φ resulting from simultaneous excitation of both windings will be represented by points having both a horizontal and vertical co-ordinate value.

The total flux Φ is important for switching purposes, but the actual differential phase of the ferrite (nominal) half–wave plate is of more interest as far as the r–f performance of the phase shifter is concerned. Since there is a well–defined mapping relationship between the two quantities, Figure 6 has been extended to show typical contours of differential phase resulting from values of total flux on the Φ–plane. The insertion loss L of the device will increase with deviation of differential phase away from the optimum 180° value, according to the relationship

$$L(\text{dB.}) = L_0 - 20 \log_{10}(\sin(\zeta/2)), \tag{5}$$

where L_0 is the minimum insertion loss of the phase shifter, and ζ is the differential phase of the (nominal) half–wave plate. Since the ferrite rod fills the waveguide, ζ will decrease monotonically with frequency and the bandwidth will be limited[7].

Polar angles on the Φ-plane and the r–f insertion phase of the device both vary in a 2:1 ratio relative to the mechanical orientation angle of the transverse fourpole magnetic bias field. Therefore it follows that the insertion phase of the unit will be in one–to–one correspondence with the angle ϕ of the operating point, relative to a properly defined reference axis on the Φ–plane.

IV. Switching Considerations

Faraday's Law states that the time rate of change of the magnetic flux Φ produced by a coil will be proportional to the available voltage (i. e. the voltage at the coil terminals after accounting for the resistive voltage drop), divided by the number of turns in the coil. That is, shorter switching times for the phase shifter require a larger voltage across the terminals of the windings, or fewer turns in the windings, or a combination of both techniques. Since the windings are supposed to create sine and cosine distributions of flux density around the periphery of the microwave ferrite rod, there is obviously a limit to the reduction of turns possible. Even when the distributions are reasonably preserved, windings with few turns will tend to produce larger phase–setting errors in the complete phase shifter over the entire range of angle–set command values. Of course, the magnetizing current will increase at shorter switching times, partly because of the reduction in turns, and partly because of the currents induced in the waveguide walls (shorted–turn damping). This latter effect is less in the case of fourpole field switching [8] than for simple solenoid switching, and is also restricted by using a thin metallization, sputtered directly on the ferrite rod, as the waveguide wall.

The ferrite rod–yoke magnetic circuit exhibits square–loop characteristics for the dependence of the total flux Φ on the magnetizing current I_m in the yoke windings. When a voltage is applied across one of the windings, I_m initially jumps to the level determined by the coercive force H_c at the remanent starting point, then increases in time as a ramp, finally "spiking" as the knee of the hysteresis loop is reached. Applying voltages V_{sin} and V_{cos} simultaneously to both the sine and cosine windings, respectively, causes the trajectory of total flux versus time to move along a line at an angle ϕ relative to the horizontal axis, where

$$\phi = \tan^{-1} (V_{sin}/V_{cos}) \tag{6}$$

The superposition of winding voltages will produce a transient mmf in the circuit that is indistinguishable from the case of a voltage on a single winding, except that the orientation of the resulting field is at the mechanical angle $\phi/2$ relative to a zero reference defined when only the cosine winding is excited. Once this fact is accepted, it does not require a great leap of faith to realize that the transient currents I_{sin} and I_{cos} in each of the two windings will simply be the components of the magnetizing current I_m given by

$$I_{sin} = I_m \sin \phi \tag{7}$$

$$I_{cos} = I_m \cos \phi \tag{8}$$

With proper construction, the configuration will exhibit

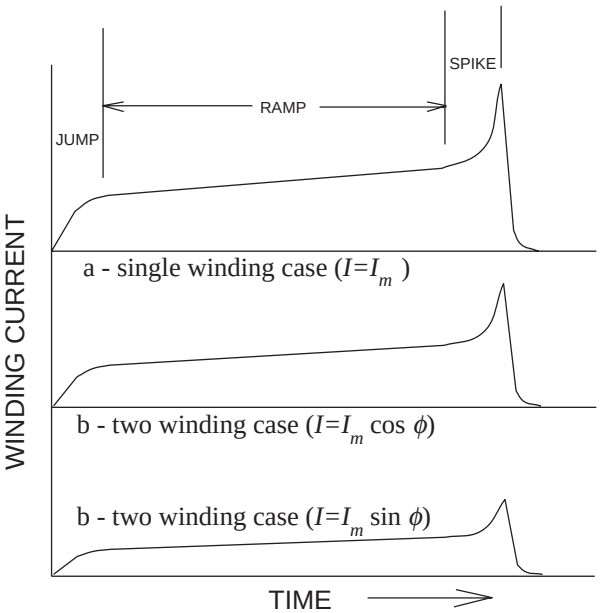

Fig. 7. Typical transient magnetizing current waveforms: a – single-winding excitation; b – simultaneous excitation in both windings. Note in case b that "spiking" occurs simultaneously in both windings, but generally at different current levels.

the same hysteresis characteristic for every choice of angular orientation of the fourpole biasing field. Figure 7 illustrates the typical waveforms observed during transient operation; note that the currents "spike" simultaneously in the two windings, although at different levels.

Like other latching ferrite phase shifters, phase states are changed by applying "Reset" and "Set" pulses in sequence, where the purpose of the "Reset" pulse is to remove information about the previous state and the purpose of the "Set" pulse is to reach the desired remanent condition for the new state. Unlike other latching ferrite phase shifters, however, the state information is contained in the ratio of voltages applied to the two windings through the relationship of equation (6) above. The total remanent flux for every state is the same, and therefore the "Reset" and "Set" pulse lengths will be the same for all states, and in fact will be similar for every phase shifter in a phased-array antenna. This fact allows the switching cycle pulse generation to be removed from the individual phase shifter drivers, and to be centrally generated and compensated for temperature and supply voltage fluctuations. Finally, because the angle setting value is determined by the mathematical relationship of equation (6), there is no need for lookup tables of "Set" pulse lengths to compensate for nonlinear dependence of phase shift versus partial magnetization level; and the phase changes have first–order independence from r–f frequency and operating temperature variations.

V. Experimental results

Several laboratory–model latching rotary-field phase shifters have been built at C–Band and S–Band in order to demonstrate and study the concepts. These models used r–f rod materials from the lithium–titanium ferrite and yttrium garnet families. Aside from material–dependent

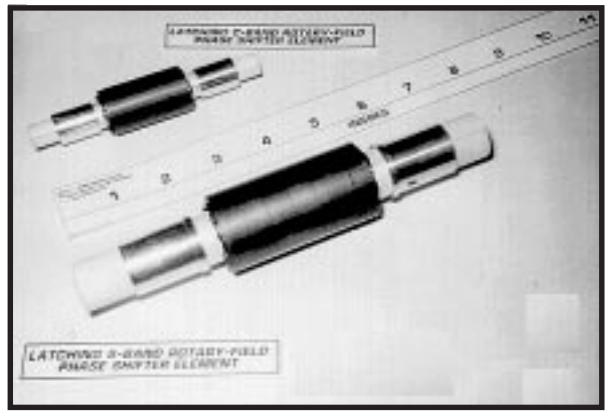

Fig. 8. Photograph of experimental C–Band and S-Band latching rotary–field phase shifters.

characteristics (e.g. peak power threshold for increased loss, insertion loss, temperature dependences) all models exhibited similar performance and control features. Figure 8 shows a photograph of devices operating in each frequency band. The C–Band experimental units had dielectric matching sections included at each end to allow coupling into standard WR137 rectangular waveguide with low return loss in the frequency range 5.4–5.9 GHz, while the S–Band units matched into WR284 rectangular waveguide over various frequency ranges from 2.85 up to 3.5 GHz. Similar dielectric coupling sections have been found suitable for direct matching as radiating elements at the aperture plane of a phased–array antenna.

Figure 9 shows a measured trace of the insertion loss envelope of a C–Band unit, made by rapidly scanning the phase shift over all states as frequency is slowly swept. This unit used an r–f ferrite of the lithium–titanium type. Figure 10 displays plots of the phase error versus phase command value at 5.4, 5.65, and 5.9 GHz. for the same C–Band unit. For these plots, the phase was commanded to 256 equally spaced values (i.e. 8–bit quantization) in a pseudo–random sequence. Phase error values were computed and recorded, then subsequently plotted as a function of phase command. Computed RMS error levels are noted for each plot. All data presented here for C–Band were measured at laboratory ambient temperature.

Figure 11 presents a measured trace of the differential

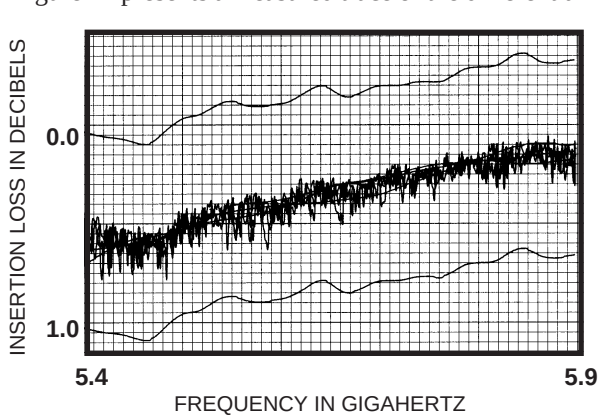

Fig. 9. Insertion loss envelope over frequency for experimental C-Band latching rotary–field phase shifter.

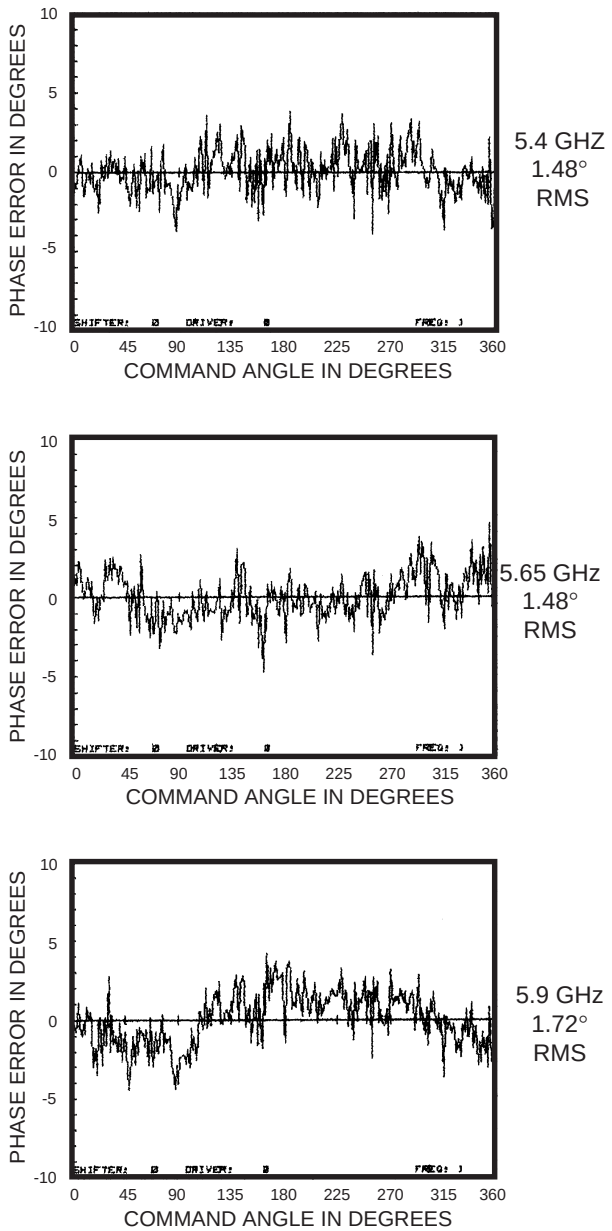

Fig. 10. Phase error vs. phase command at selected frequencies for experimental C–Band latching rotary–field phase shifter.

phase hysteresis characteristic of an S–Band device using a lithium–titanium type r–f ferrite. This curve was made by re–aligning the quarter–wave plates and the drive stator such that linear polarization propagated through the r–f ferrite section, using excitation of a single coil of the stator. Figures 12 and 13 show plots of the average insertion loss and rms phase error variation over a range of ambient temperatures, for a different S–Band model using an yttrium garnet type rod material. The increase of r–f loss with decreasing temperature below 50° C occurs because the magnetic activity and magnetic loss of the garnet material both increase with decreasing temperature. Above 50° C, the garnet rod is not long enough to give the full half-wave plate differential phase, and so the loss increases with increasing temperature as the magnetic activity decreases further. Except at the lowest temperatures, the rms phase error remains the same, as

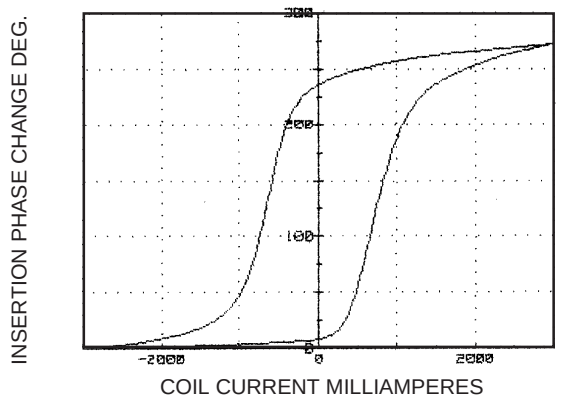

Fig. 11. Differential phase hysteresis characteristic for experimental S–Band latching rotary-field phase shifter.

expected.

The garnet material and r–f configuration used in this latter experimental unit were identical to that used in nonlatching rotary–field phase shifters designed to operate at peak power levels of 35 KW. and average power levels of 800 watts. There is no question that the peak power to reach nonlinear threshold effects would be the same for a latching unit; however, the average power handling capability is reduced, because the thermal con-

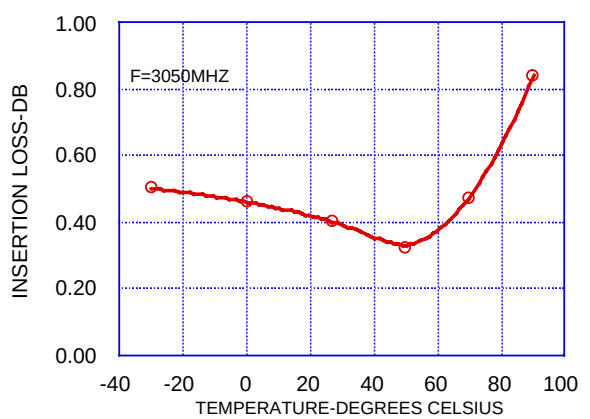

Fig. 12. Insertion loss vs. temperature characteristic of experimental S–Band phase shifter.

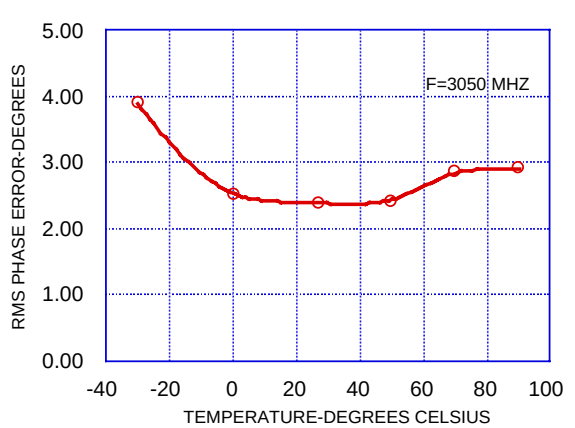

Fig. 13. RMS phase error vs. temperature characteristic of experimental S–Band phase shifter.

ductivity of the ferrite drive yoke is smaller than that of the metal drive stator of a nonlatching version. Measurements on the garnet rod temperature rise versus average power indicate that a level of 200 watts can be accommodated, which is one–fourth the average power level that can be handled by a nonlatching design using the same garnet material. Finally, the weight of the C–Band devices was about 100 grams, while the S–Band units varied from about 295 (low peak power) to 435 (high peak power) grams, without including housing.

VI. Conclusions

Latching rotary–field phase shifters have been demonstrated at C–Band and S–Band, and should be achievable at L–Band and X–Band. These devices exhibit most of the desirable characteristics of the nonlatching version, plus some unanticipated additional features:

(a) Low insertion loss
(b) Minimal frequency dependence of phase changes
(c) Minimal temperature dependence of phase changes
(d) High peak power handling capability
(e) State–independent RESET–SET pulse lengths
(f) Lookup tables for calibration not required
(g) Faster switching than nonlatching version
(h) No quiescent current needed.

VI. ACKNOWLEDGMENT

It is a pleasure to acknowledge the assistance of the author's colleagues at Microwave Applications Group, including many helpful discussions aimed at exploring and understanding the characteristics of the latching ferrite rotary–field phase shifter, and with special thanks to Dr. William E. Hord and Mr. Charles M. Oness.

VII. References

[1] A. G. Fox,"An adjustable waveguide phase changer," *Proc. IRE*, vol. 35, pp. 1489–1498, Dec. 1947.

[2] J. Cacheris,"Microwave single–sideband modulator using ferrites," *Proc. IRE*, vol 42, pp. 1242–1247, Aug. 1954.

[3] N. B. Sultan,"Generalized theory of waveguide differential phase sections and application to novel ferrite devices," *IEEE Trans. Microwave Theory Tech.*, vol 19, pp. 348–357, April 1971.

[4] C. R. Boyd, Jr.,"An accurate analog phase shifter," *1971 IEEE G–MTT Int'l Symposium Digest*, pp. 104–105, May 1971.

[5] C. R. Boyd and G. Klein,"A precision analog duplexing phase shifter," *1972 IEEE G–MTT Int'l Symposium Digest*, pp. 248–250, May 1972.

[6] C. M. Oness, W. E. Hord, C. R. Boyd, Jr.,"Medium power s–band rotary field phase shifters," *1986 IEEE MTT–S Int'l Symposium Digest*, pp. 539–542, June 1986.

[7] C. R. Boyd, Jr., "Design of ferrite differential phase shift sections" *1975 IEEE MTT–S Int'l Symposium Digest*, pp. 240–242, May 1975.

[8] W. E. Hord, C. R. Boyd, Jr. and D. Diaz,"A new type of fast switching dual-mode ferrite phase shifter" *1987 IEEE MTT-S International Symposium Digest*, vol. II, pp. 985–988, June, 1987.